

SUPPORTING INFORMATION

**Mechanistic role of support-catalyst interface in electrocatalytic water reduction by
Co₃O₄ supported nanocarbon florets**

Jayeeta Saha^{†a}, Ranadeb Ball^{†a}, Ananya Sah^a, Vishwanath Kalyani^a, Chandramouli Subramaniam^{*a}

Department of Chemistry, Indian Institute of Technology, Powai, Mumbai, Maharashtra 400076, India.

Table of Contents

Serial No.	Title	Page No.
Figure S1	SEM and TEM image of DFNS	3
Figure S2	SEM image and Surface area plot of DFNS	4
Table S1	Summary of SSA of different nanocarbons	5
Figure S3	SEM image of -NCF	6
Figure S4	TEM image of Co ₃ O ₄ -NCF	6
Figure S5	TGA, Raman spectroscopy and XPS of Co ₃ O ₄ -NCF	7
Figure S6	SEM and TEM image of pure Co ₃ O ₄	8
Figure S7	XRD, XPS and Raman spectroscopy of pure Co ₃ O ₄	9
Figure S8	Electrochemical data of Co ₃ O ₄ -NCF in acidic (H ₂ SO ₄) medium	10
Table S2	Electrochemical comparison of Co ₃ O ₄ -NCF and pure Co ₃ O ₄	10
Table S3	Summary of electrochemical parameter of different catalysts	11
Table S4	Summary of SSA and capacitive double layer with different catalysts	12
Figure S9	Schematic representation of operand setup	13
Figure S10	Operando Raman spectra of Co ₃ O ₄ -NCF in basic condition with applied potential	14
Figure S11	Operando Raman spectra of Co ₃ O ₄ -NCF in acidic condition with applied potential	15
Figure S12	Comparison of CV of Co ₃ O ₄ -NCF with Pt and graphite electrode	16
Figure S13	Redox behaviour of Co ₃ O ₄ -NCF in acidic and basic medium	17
Table S5	ICP-AES analysis of acid treated Co ₃ O ₄ -NCF	17
Figure S14	Comparison of XPS: before and after electrochemistry	18
Figure S15	Time resolved in-situ Raman spectro-electrochemical study of Co ₃ O ₄ -NCF in heavy water (D ₂ O) for aHER at -0.4V (vs RHE)	19
Figure S16	Electrochemical data of Co ₃ O ₄ -NCF in acidic (HClO ₄) medium	19
Scheme S1	Proposed mechanism of HER with Co ₃ O ₄ -NCF	20
References	References	20

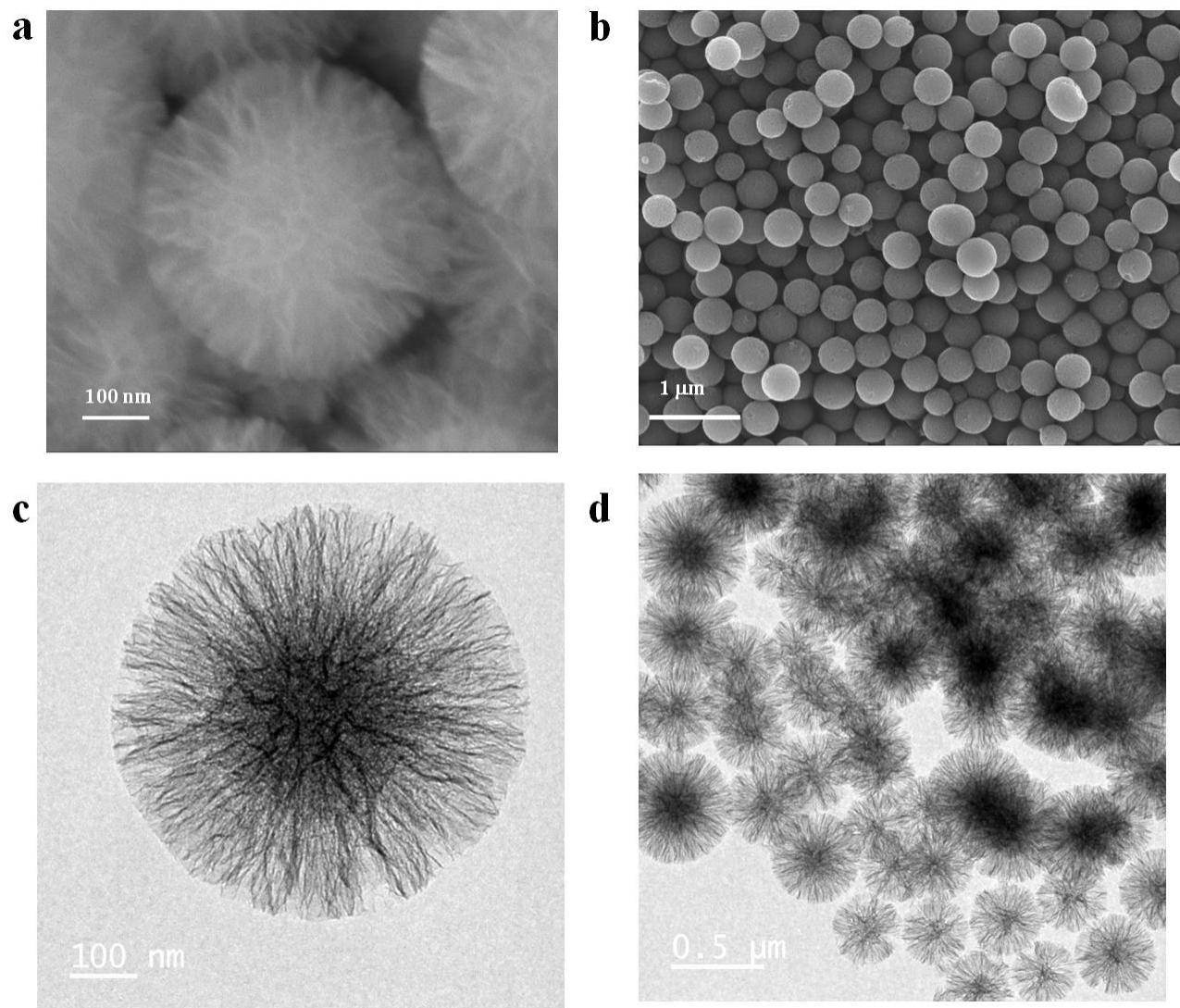


Figure S1. (a,b) SEM images and (c,d) TEM image of DFNS.

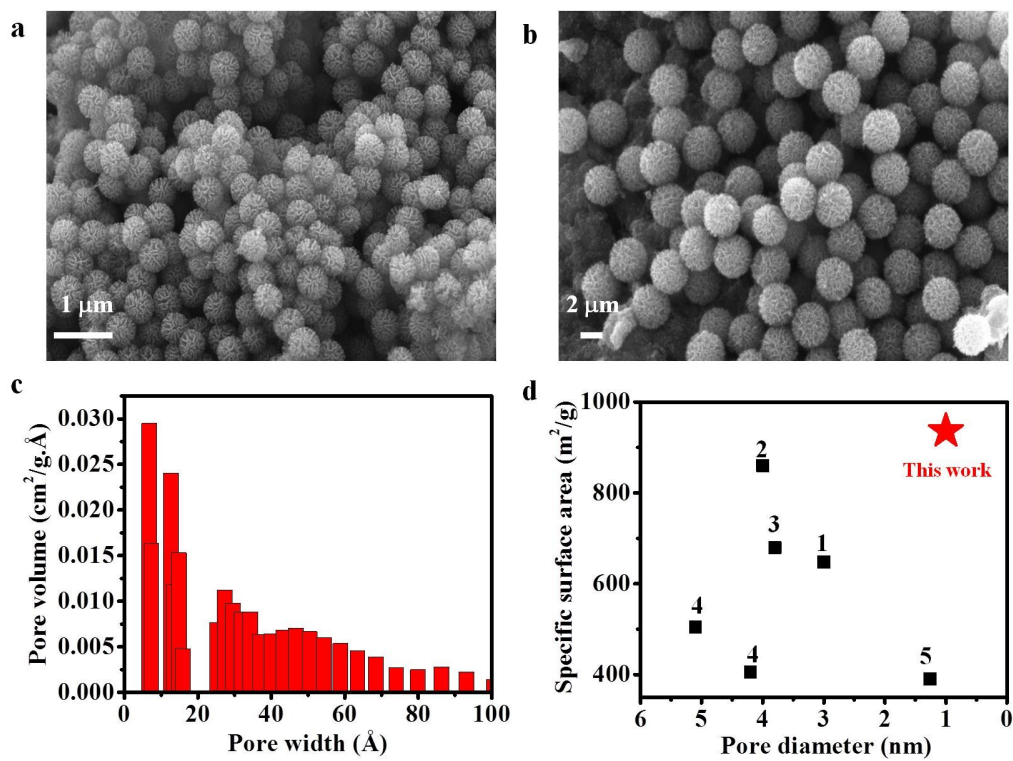


Figure S2. (a, b) SEM images of NCF. (c) Pore-width distribution of NCF. (d) Ashby plot of SSA with pore diameter with different material.¹⁻⁵

Table S1. Summary of specific surface area and pore diameter of various carbon materials

Serial No.	Material	Specific surface area (m²/g)	Pore diameter (nm)	References
1	Nanocarbon floret (NCF)	936	< 1	This work
2	Carbon hollow spheres	648	3	1
3	HMCSs	769.5	3.8	3
4	HCSs	88	-	6
5	Annealed HCSs	328	-	
6	Hollow carbon nanospheres	42	-	7
7	Mesoporous Carbons	200	20-50	8
8	Hollow carbon sphere	860	2-4	2
9	N-doped hollow mesoporous carbon	504	5.1	4
10	Hollow carbon sphere	390	1.26	5
11	Activated porous carbon	405	4.2	9
12	Co-m-NC	342	4.7	10
13	MCN	596	-	11
14	HMC	340	-	12

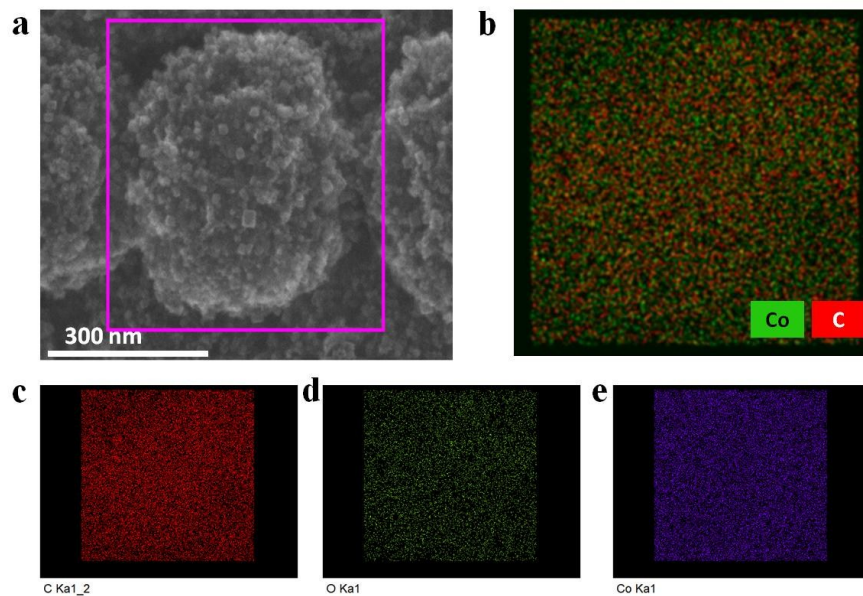


Figure S3. (a) SEM image and (b) composite mapping of Co (green) and C (red) of $\text{Co}_3\text{O}_4\text{-NCF}$. Individual mapping of (c) C, (d) O and (e) Co.

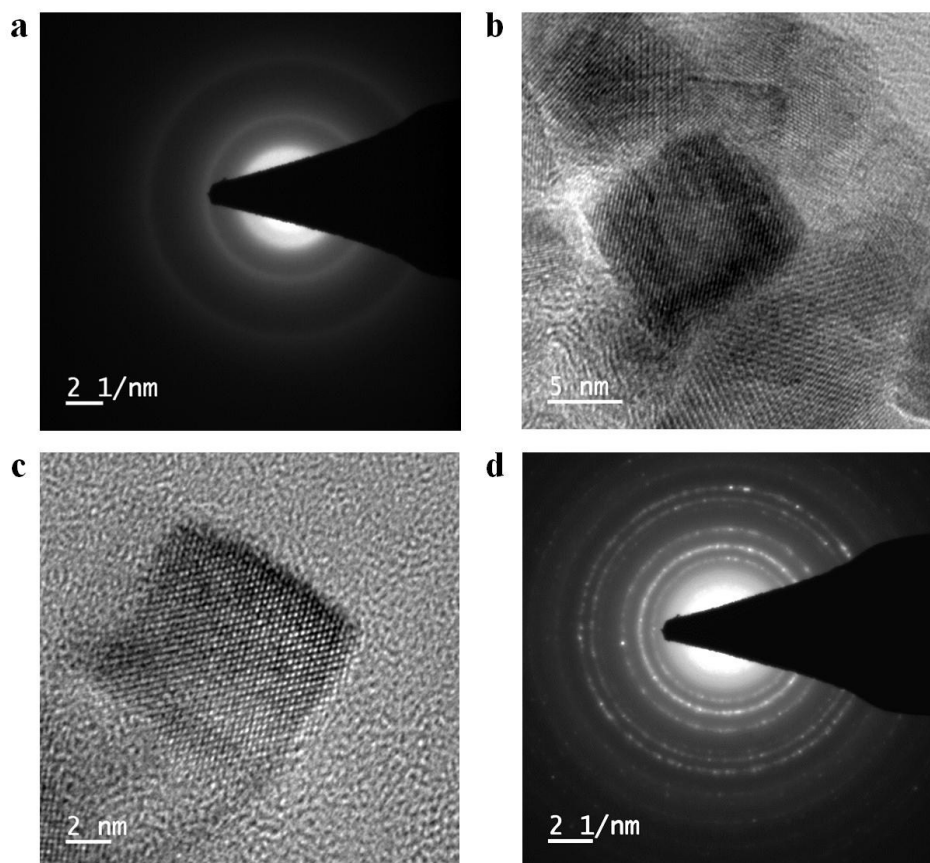


Figure S4. SAED pattern of (a) pristine NCF and (b, c) HRTEM and (d) SAED pattern of $\text{Co}_3\text{O}_4\text{-NCF}$.

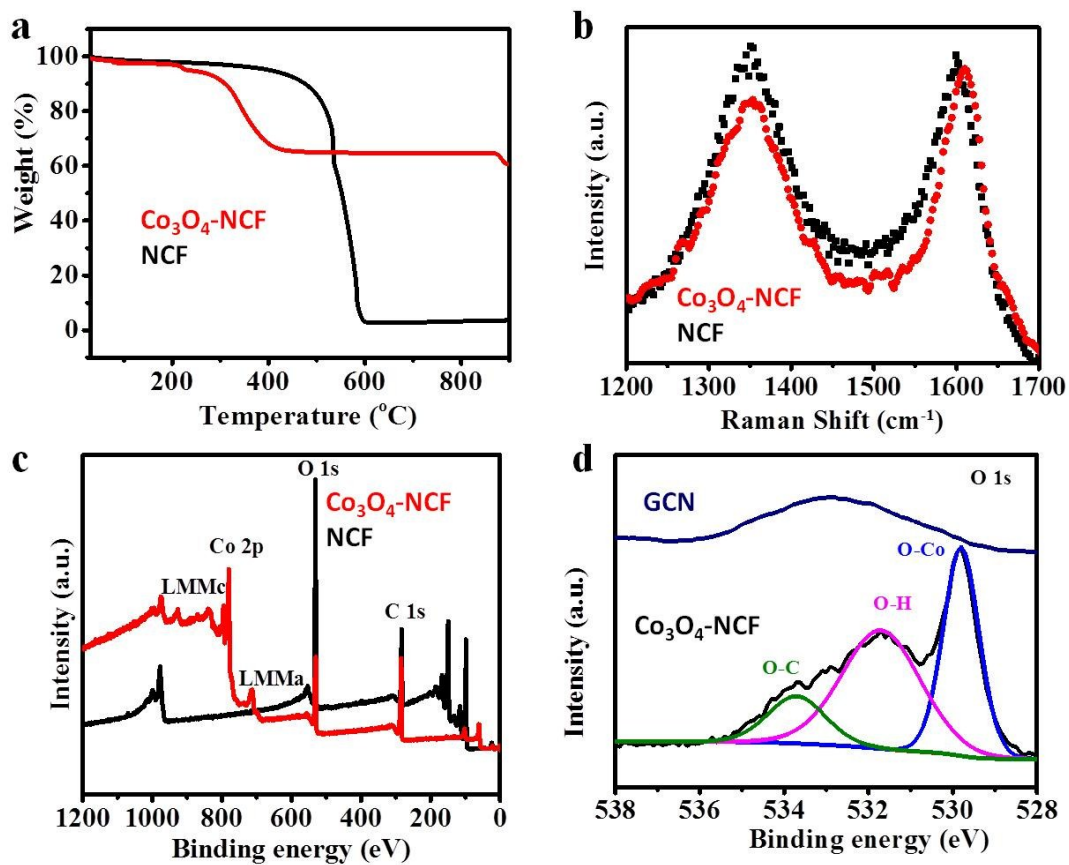


Figure S5. (a) Thermo-gravimetric analysis (TGA) of pristine NCF and $\text{Co}_3\text{O}_4\text{-NCF}$. (b) Raman spectra of pristine NCF and $\text{Co}_3\text{O}_4\text{-NCF}$ (c) XPS of pristine NCF and $\text{Co}_3\text{O}_4\text{-NCF}$. (d) O 1s XPS of NCF and deconvolution of O 1s XPS of $\text{Co}_3\text{O}_4\text{-NCF}$.

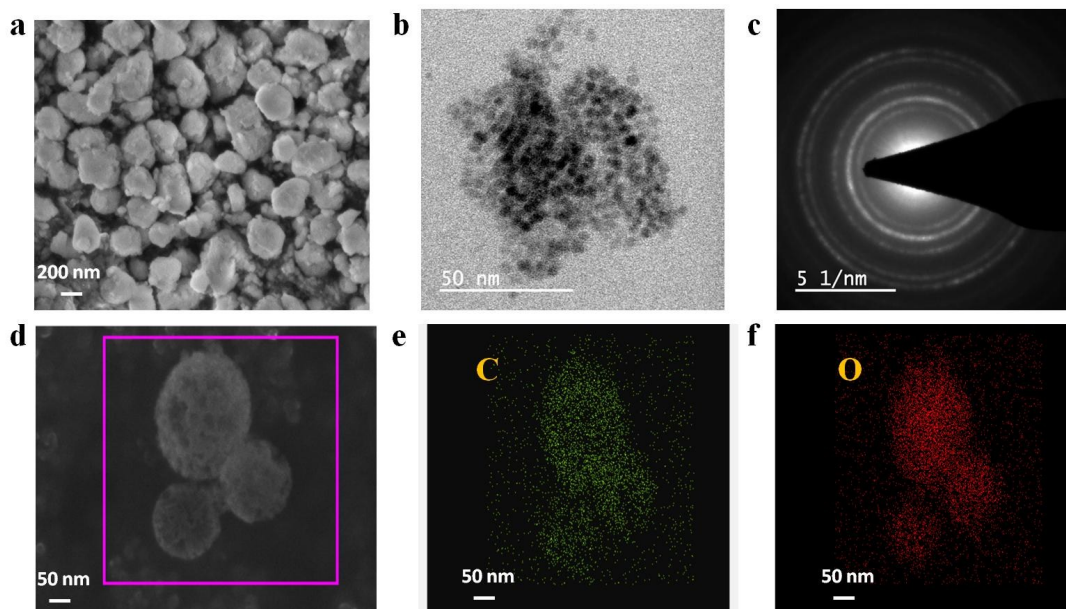


Figure S6. (a) SEM and (b) TEM image of pure Co_3O_4 prepared without NCF. (c) SAED pattern of pure Co_3O_4 . (d) EDS mapping of pure Co_3O_4 , (e) Carbon mapping and (f) Oxygen mapping.

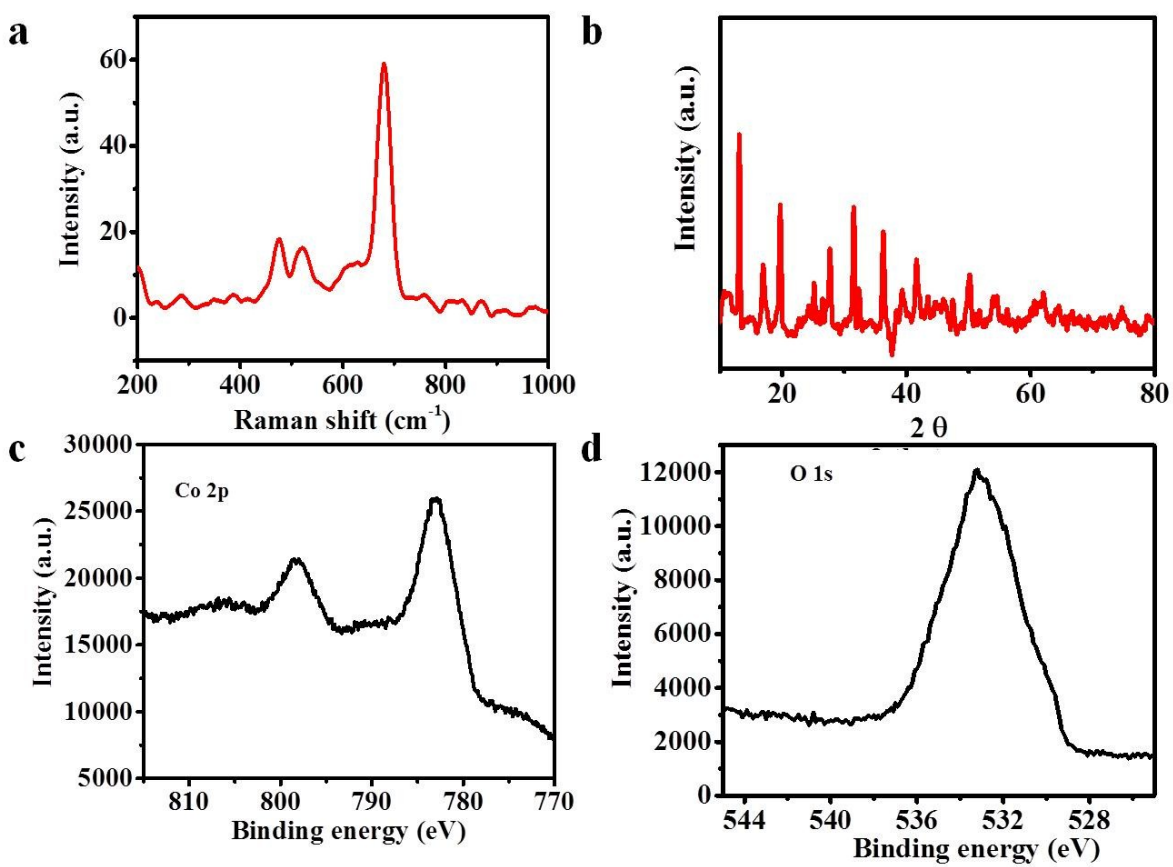


Figure S7. (a) Raman spectra, (b) XRD, (c) Co 2p XPS and (d) O 1s XPS of pure Co_3O_4 .

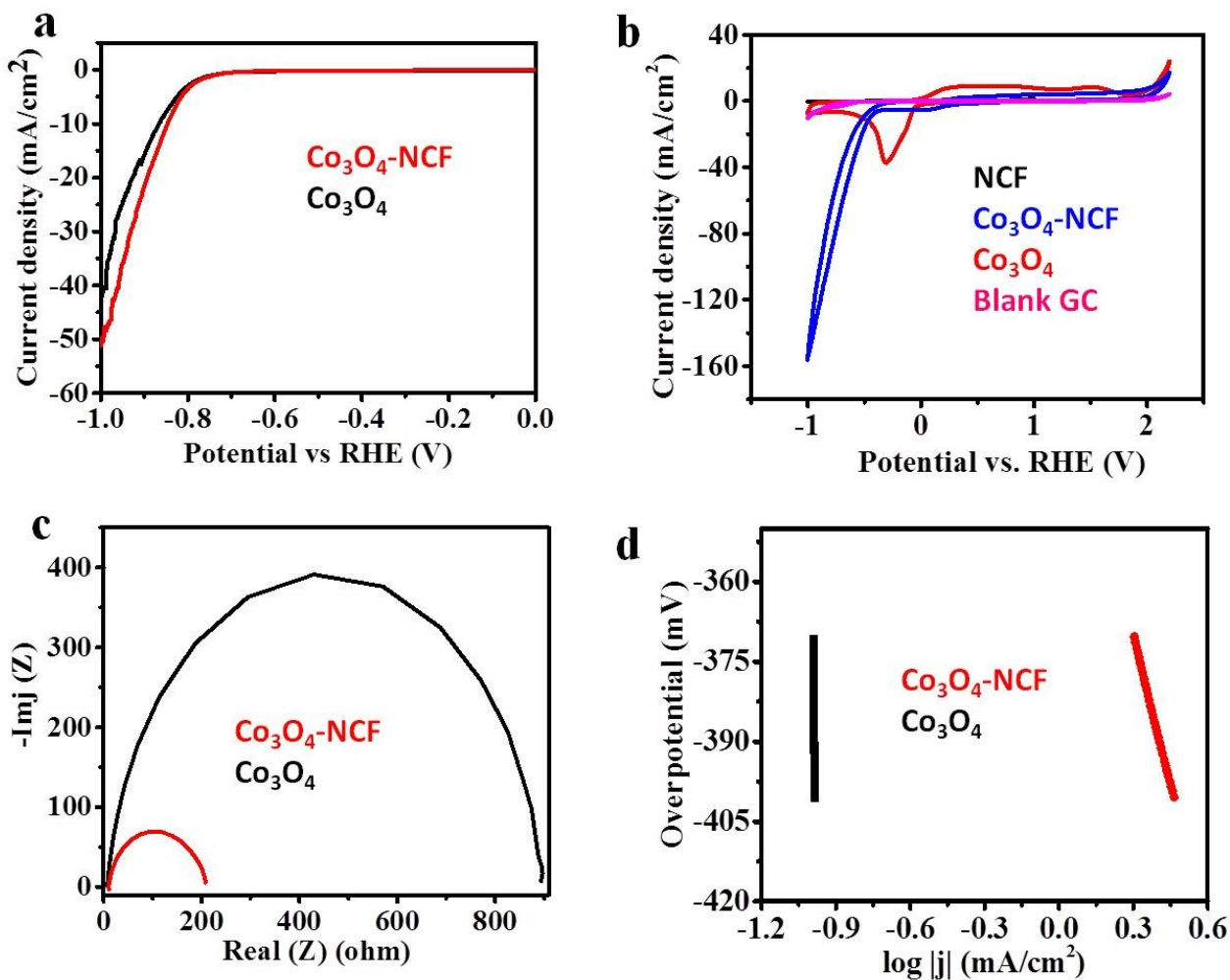
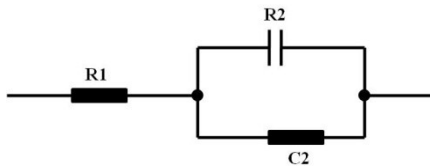


Figure S8. (a) Linear sweep voltammetry in 0.5 M H_2SO_4 (pH=0.5) of pure Co_3O_4 and $\text{Co}_3\text{O}_4\text{-NCF}$ (scan rate= 2 mV/s). (b) Cyclic voltammetry in 0.5 M H_2SO_4 (pH=0.5) of blank glassy carbon (GC), pristine NCF, pure Co_3O_4 and $\text{Co}_3\text{O}_4\text{-NCF}$ (scan rate= 100 mV/s). (c) Nyquist plots of pure Co_3O_4 and $\text{Co}_3\text{O}_4\text{-NCF}$. (d) Tafel plots of pure Co_3O_4 and $\text{Co}_3\text{O}_4\text{-NCF}$.

Tafel slope calculation

The current density (j) vs overpotential (t) data obtained from LSV (2 mV/s) were transformed into overpotential (t) vs $\log(|j|)$. Further, the overpotential varied linearly as a function of $\log(|j|)$ from $\log(|j|)=0$ to 1 (1 corresponds to $j=10 \text{ mA/cm}^2$). The slope of the function was obtained using linear fit having $R^2=0.998$, which gives the Tafel slope (mV/dec) for HER in alkaline and acidic medium.

Table S2. Equivalent circuit extracted circuit parameters for different systems investigated.



Catalyst	Medium	R1 Electrolyte Resistance (ohm)	R2 Charge transfer resistance (ohm)	C _{dl} double layer capacitance (mF/cm ²)
Pure Co ₃ O ₄	0.5 M H ₂ SO ₄	7.887	846.4	42
Co ₃ O ₄ -NCF	0.5 M H ₂ SO ₄	10.74	170.5	190
Pure Co ₃ O ₄	1 M KOH	14.04	350.9	36.5
Co ₃ O ₄ -NCF	1 M KOH	16.39	35.8	410
Pure Co ₃ O ₄	0.5 M HClO ₄	37.98	1986	31
Co ₃ O ₄ -NCF	0.5 M HClO ₄	57.27	80	75

Table S3. Summary of electrochemical parameters of some reported catalysts

Serial No.	Catalyst	Medium	Overpotential (mV)	Current density (mA/cm ²)	Tafel slope (mV/dec)	Reference (SI)
1	Co ₃ O ₄ -NCF	1 M KOH	460	10	119	This work
2	Co ₃ O ₄ -NCNT	1 M KOH	350	10	-	13
3	Co ₃ O ₄ -carbon paper	1 M KOH	350	16.5	115	14
4	Co ₃ O ₄ -calcinated carbon	1 M KOH	350	8.5	198	14
5	CoO _x -CC	1 M KOH	193	20	-	15
6	U-CNT-900	1 M KOH	240	10	-	16
7	Co ₃ O ₄ -Ni foam	1 M KOH	50	1	-	17

Table S4. Summary of SSA and C_{dl} of recently reported materials

Serial No.	Materials	SSA (m ² /g)	C _{dl} (mF/cm ²)	Reference
1	Metal-N-C (M=W, Mo, Cr, Mn, Fe, Co, Ni, Cu, Zn)	712-382	-	18
2	Co ₃ O ₄ -NCNT	37	-	13
3	CoO _x -CNT-CC	88	1155	15
4	Co ₃ O ₄ -NCF	646	410	This work

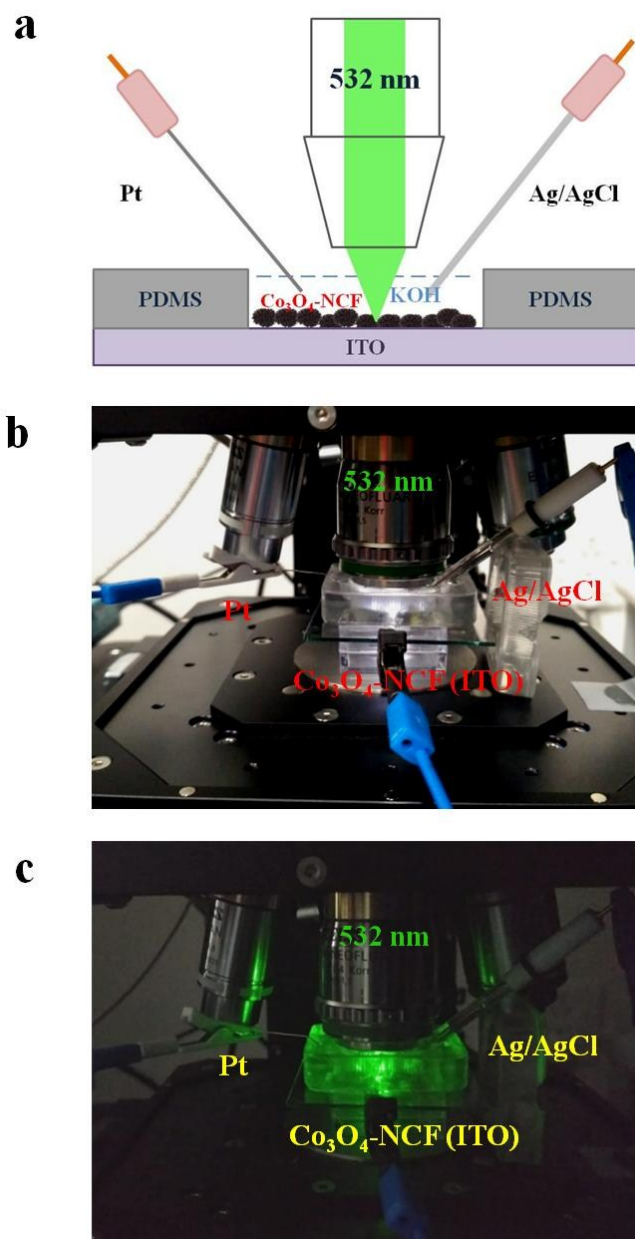


Figure S9. (a) Schematic representation of the operando Raman setup. Photograph of customized operando Raman setup with laser on (b) and laser off (c).

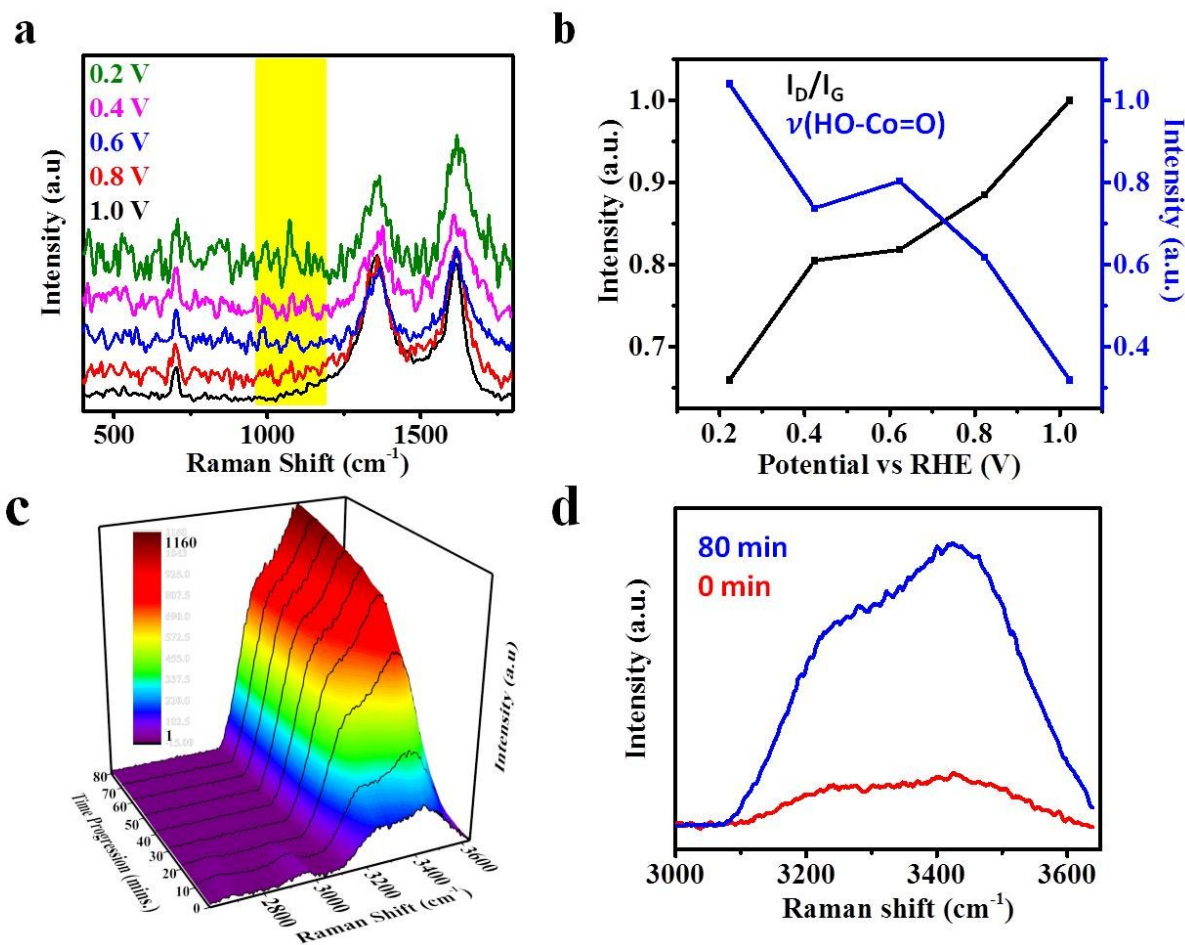


Figure S10. (a) Operando Raman spectra of $\text{Co}_3\text{O}_4\text{-NCF}$ in 1 M KOH with different applied potential. (b) Evolution of I_D/I_G (blue) and HO-Co=O (black) in 1 M KOH.² (c) Operando Raman spectroscopy of HER at 0.8 V (vs RHE) in 1 M KOH using $\text{Co}_3\text{O}_4\text{-NCF}$ catalyst (region 2600-3600 cm^{-1}). (d) Raman spectroscopy of HER at 0.8 V (vs RHE) in 1 M KOH using $\text{Co}_3\text{O}_4\text{-NCF}$ catalyst (region 2600-3600 cm^{-1}) at 0 min (red) and 80 min (blue).

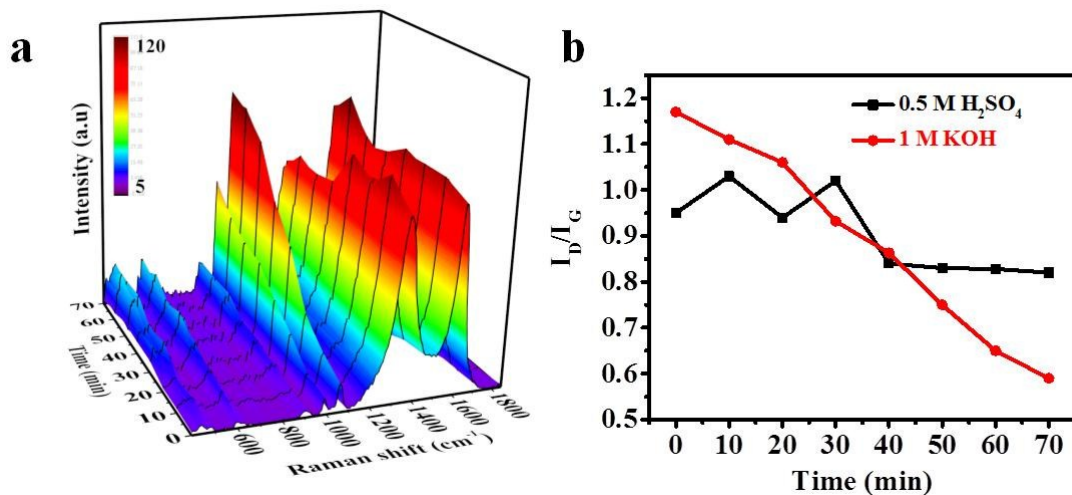


Figure S11. (a) Operando Raman spectroscopy of HER at 0.2 V (vs RHE) in 0.5 M H₂SO₄ using Co₃O₄-NCF catalyst. (b) Spectral evolution of I_D/I_G with time in 0.5 M H₂SO₄ (black) and 1 M KOH (red).

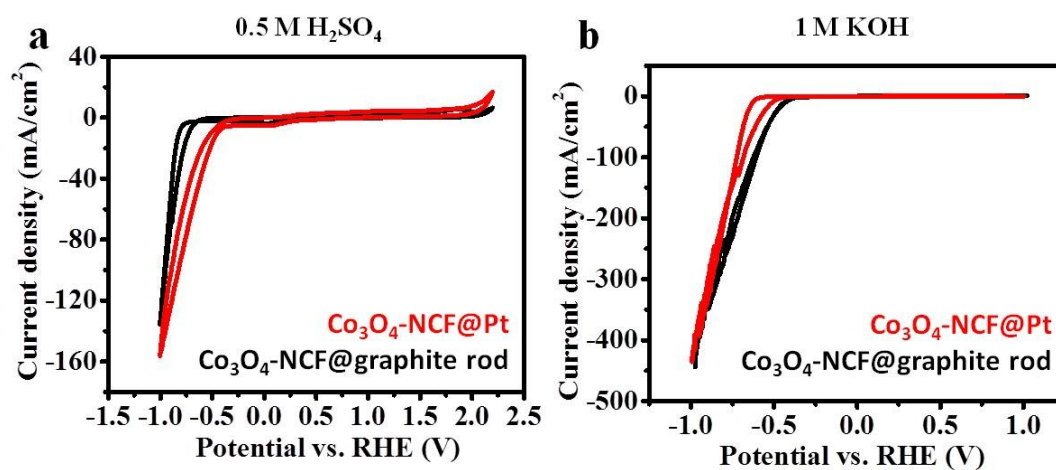


Figure S12. Comparison CV of Co₃O₄-NCF with different counter electrodes (graphite rod and Pt) in both (a) acidic and (b) alkaline pH.

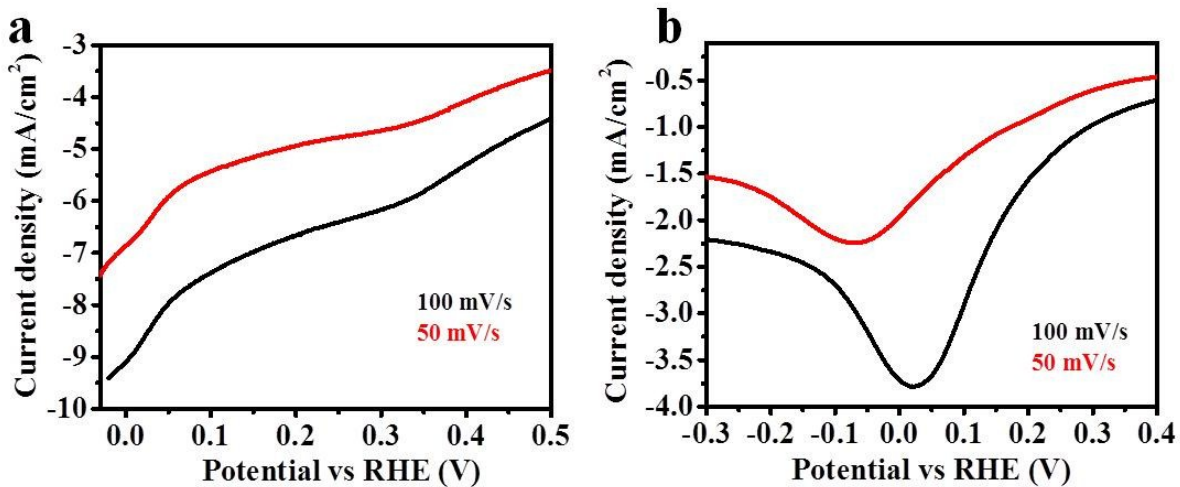


Figure S13. Cyclic voltammogram (CV) of $\text{Co}_3\text{O}_4\text{-NCF}$ in (a) basic medium and (b) acidic medium.

Table S5. ICP-AES analysis of acid treated $\text{Co}_3\text{O}_4\text{-NCF}$

Sample	Concentration of Cobalt (ppm)
$\text{Co}_3\text{O}_4\text{-NCF}$ in H_2SO_4	> 140

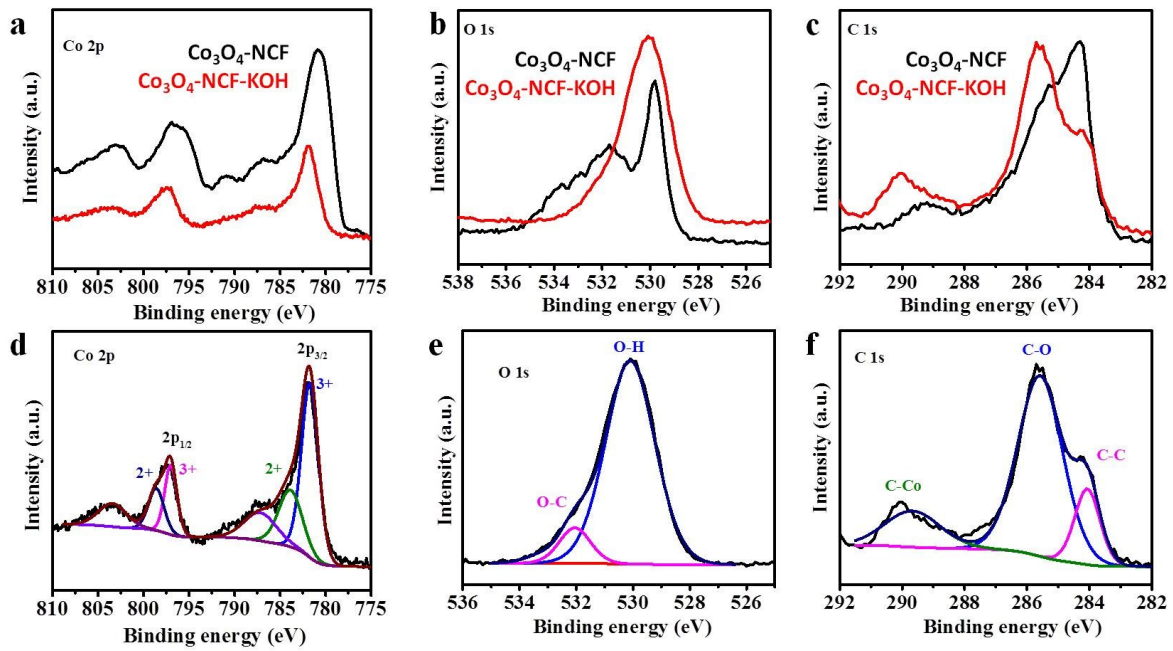


Figure S14. Comparison of (a) Co 2p, (b) O 1s and (c) C 1s XPS of Co₃O₄-NCF before and after HER in 1 M KOH. Decovoluted (d) Co 2p, (e) O 1s and (f) C 1s XPS of Co₃O₄-NCF after HER in 1 M KOH.

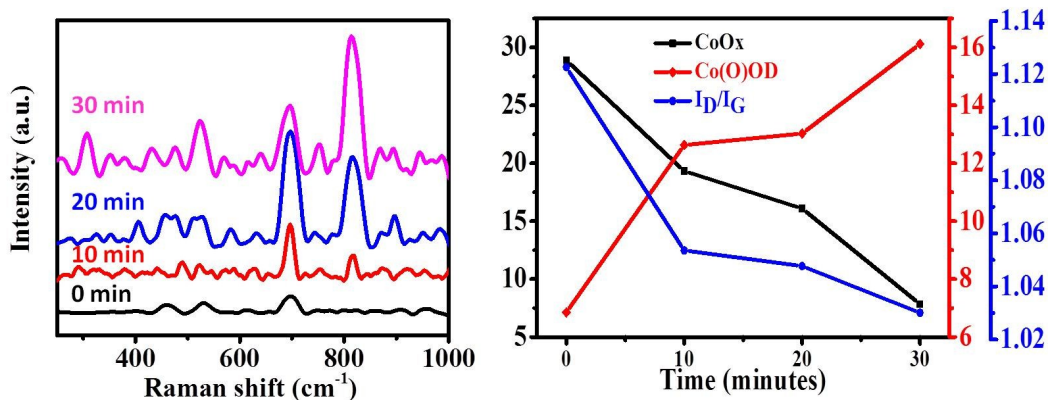


Figure S15. a) Time resolved in-situ Raman spectro-electrochemical study of Co_3O_4 -NCF in heavy water (D_2O) for a)HER and b) Intensity of Co-OOD peak (815 cm^{-1}), Co-O_x (699 cm^{-1}) and I_D/I_G at -0.4V (vs RHE) with time under in-situ conditions.

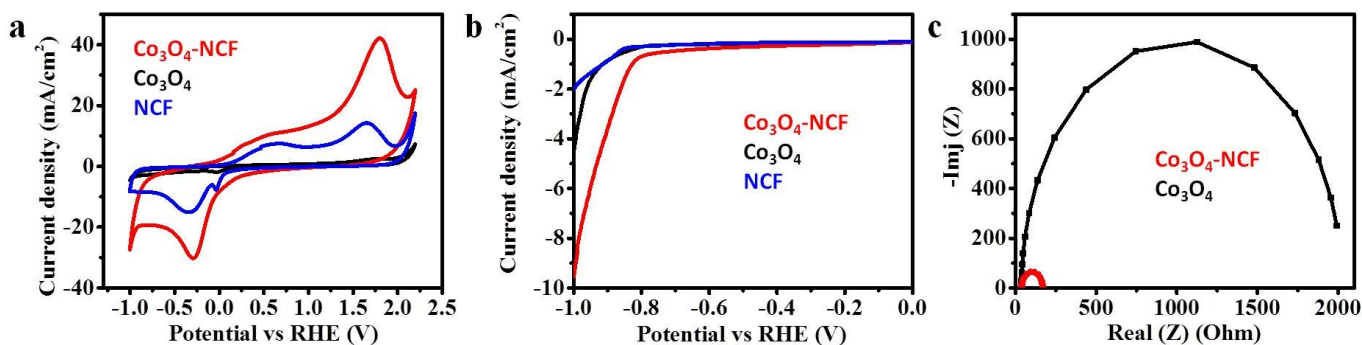
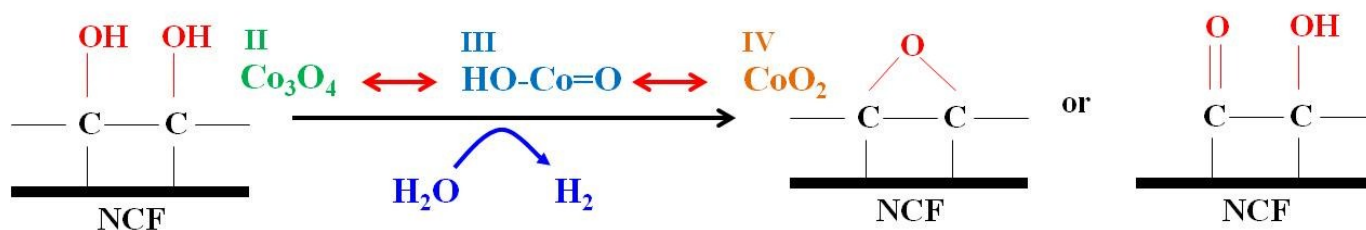


Figure S16. a) Cyclic voltammetry in 0.5 M HClO_4 of pristine NCF, pure Co_3O_4 and Co_3O_4 -NCF (scan rate= 100 mV/s). (b) Linear sweep voltammetry in 0.5 M HClO_4 pristine NCF, pure Co_3O_4 and Co_3O_4 -NCF (scan rate= 2 mV/s). (c) Nyquist plots of pure Co_3O_4 and Co_3O_4 -NCF.



Scheme S1. Proposed mechanism of HER at Co_3O_4 -NCF surface.

Reference

- 1 T. R. Hellstern, J. Kibsgaard, C. Tsai, D. W. Palm, L. A. King, F. Abild-Pedersen and T. F. Jaramillo, *ACS Catal.*, 2017, **7**, 7126–7130.
- 2 Z. Jiang, Z. J. Jiang, T. Maiyalagan and A. Manthiram, *J. Mater. Chem. A*, 2016, **4**, 5877–5889.
- 3 Y. Li, H. Wang, L. Xie, Y. Liang, G. Hong and H. Dai, *J. Am. Chem. Soc.*, 2011, **133**, 7296–7299.
- 4 H. Zhang, X. Liu, Y. Wu, C. Guan, A. K. Cheetham and J. Wang, *Chem. Commun.*, 2018, **54**, 5268–5288.
- 5 Y. Liang, Y. Li, H. Wang, J. Zhou, J. Wang, T. Regier and H. Dai, *Nat. Mater.*, 2011, **10**, 780–786.

- 6 S. Zhang, X. Yu, F. Yan, C. Li, X. Zhang and Y. Chen, *J. Mater. Chem. A*, 2016, **4**, 12046–12053.
- 7 C. Huang, T. Ouyang, Y. Zou, N. Li and Z. Q. Liu, *J. Mater. Chem. A*, 2018, **6**, 7420–7427.
- 8 S. Du, Z. Ren, J. Zhang, J. Wu, W. Xi, J. Zhu and H. Fu, *Chem. Commun.*, 2015, **51**, 8066–8069.
- 9 H. S. Ahn and T. D. Tilley, *Adv. Funct. Mater.*, 2013, **23**, 227–233.
- 10 L. Hadidi, E. Davari, M. Iqbal, T. K. Purkait, D. G. Ivey and J. G. C. Veinot, *Nanoscale*, 2015, **7**, 20547–20556.
- 11 F. Hu, H. Yang, C. Wang, Y. Zhang, H. Lu and Q. Wang, *Small*, 2017, **13**, 1–8.
- 12 J. Wei, Y. Liang, X. Zhang, G. P. Simon, D. Zhao, J. Zhang, S. Jiang and H. Wang, *Nanoscale*, 2015, **7**, 6247–6254.
- 13 X. Zou, X. Huang, A. Goswami, R. Silva, B. R. Sathe and T. Asefa, *Angew. Chemie - Int. Ed.*, 2014, **53**, 4372–4376.
- 14 J. Wan, W. Chen, C. Chen, Q. Peng, D. Wang and Y. Li, *Chem. Commun.*, 2017, **53**, 12177–12180.
- 15 J. Wang, Z. Wei, H. Wang, Y. Chen and Y. Wang, *J. Mater. Chem. A*, 2017, **5**, 10510–10516.
- 16 K. Zhang, Y. Zhao, D. Fu and Y. Chen, *J. Mater. Chem. A*, 2015, **3**, 5783–5788.
- 17 A. J. Esswein, M. J. Mcmurdo, P. N. Ross, A. T. Bell and T. D. Tilley, *J. Phys. Chem. C*, 2009, **113**, 15068–15072.
- 18 A. Morozan, V. Goellner, Y. Nedellec, J. Hannauer and F. Jaouen, *J. Electrochem. Soc.*, 2015, **162**, H719–H726.